

FEATURES OF CALCULATING THE DESCENT VELOCITY OF THE LOWER BOUNDARY OF THE NEAR-CEILING LAYER IN A FIRE IN AN ATRIUM

S. V. Puzach and Nguen Tkhan' Xai

UDC 614.841

Results of calculating the dynamics of descent of the lower boundary of the near-ceiling gas layer in a model atrium using various zone approaches and a field model are presented. Comparison with experimental data is made. It is shown that when a zone mathematical model is used it is necessary to take account of the shape of the convective column formed above the source of combustion. It is pointed out that the application of the approximation of an unrestricted buoyant plume to describing parameters of the convective column does not reflect the actual thermodynamic picture of the fire development (primarily the effect of the atrium ceiling) and can lead to both an understatement and an overstatement of the fire danger of atria.

Keywords: fire, atrium, near-ceiling gas layer, heat and mass transfer, thermal gasdynamics, field mathematical model, mathematical zone model, convective column, combustion, buoyant plume.

Introduction. Actual physicochemical processes occurring in a fire in an atrium are complex, unsteady, three-dimensional, experimentally unstudied heat and mass transfer processes. The question as to the accuracy and reliability of the method of calculating heat and mass transfer is the key one in ensuring the safety of people, selecting parameters and places of location of the sensors of fire and explosion safety systems, and conducting efficient antifire measures.

The velocity of descent of the near-ceiling gas layer is primarily determined by the mass flow rate of the mixture arriving from the convective column at the indicated layer. Here the main assumption is that the convective column above the source of combustion is an unrestricted buoyant plume. However, as shown in [1, 2], the ceiling effect requires further investigations.

Zone Model of Calculating Heat and Mass Transfer in a Fire. Use is made of a three-zone model in which the room volume is split into zones of the convective column, near-ceiling gas layer, and cold air [3]. Unlike the predictive technique [3], it is taken into account that the lower boundary of the near-ceiling gas layer can be below the upper section of an opening. A similar case is considered, for example, in [4].

The basic diagram of heat and mass transfer in a room for a three-zone model is given in Fig. 1. The arrows show directions of the gas-mixture flow and the heat fluxes.

The mass flow rates and average temperatures of the gas mixture in cross sections of the convective column are determined using two approaches: 1) a point source of heat release is below the surface of a combustible material (a semiempirical calculational method [3, 5]) and 2) a distributed source of heat release is above the surface of a combustible material (empirical [6] and semiempirical methods [1, 2]). In the first case [3, 5],

$$G = 0.21 \left[\frac{g \rho_0^2 Q_{\text{fire}} (1 - \chi)}{c_p T_0} \right]^{1/3} (z + z_{\text{f.s}})^{5/3}, \quad (1)$$

$$T_{\text{av.col}} = T_0 + \frac{Q_{\text{fire}} (1 - \chi)}{c_p G}. \quad (2)$$

With the second approach, the mass flow rate in the cross section of the convective column in the case of applying an empirical method is [6]

Academy of State Fire-Prevention Service, Ministry for Emergency Situations of Russia, 4 Boris Galushkin Str., Moscow, 129366, Russia. Translated from Inzhenerno-Fizicheskii Zhurnal, Vol. 83, No. 5, pp. 885–891, September–October, 2010. Original article submitted June 22, 2009.

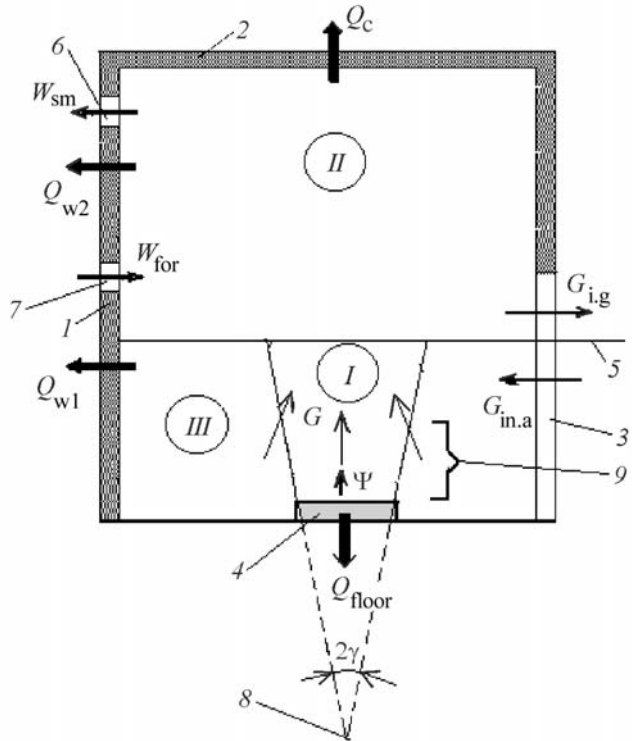


Fig. 1. Calculational scheme for heat and mass transfer in a room: 1) walls, 2) ceiling, 3) opening, 4) combustible material, 5) neutral plane (lower boundary of the near-ceiling layer), 6) smoke removal system, 7) forced ventilation system, 8) point "fictitious" heat source, 9) height of the flame zone; *I*, zone of the convective column; *II*, zone of the heated, smoke-filled, near-ceiling layer; *III*, zone of cold air.

$$z > z_{fl} : G = 0.071 \left(\frac{Q_{fire}(1-\chi)}{1000} \right)^{1/3} z^{5/3} + 1.8 \cdot 10^{-6} Q_{fire}(1-\chi), \quad (3)$$

$$z \leq z_{fl} : G = 0.032 \left(\frac{Q_{fire}(1-\chi)}{1000} \right)^{3/5} z, \quad (4)$$

where $z_{fl} = 0.166 \left(\frac{Q_{fire}(1-\chi)}{1000} \right)^{2/5}$ is the height of the flame zone, m.

When a semiempirical method [1, 2] is used, the mass flow rate is determined by solving the differential equation

$$\frac{dG}{dz} = \frac{Bz(r+z\tan\gamma)^4}{T_0AG(GT_0+Bz)} + \frac{2G\tan\gamma}{r+z\tan\gamma} - \frac{B}{T_0} \left(1 - \frac{2z\tan\gamma}{r+z\tan\gamma} \right). \quad (5)$$

The average temperature in the cross section of the convective column is obtained from Eq. (2). The height of the lower boundary of the near-ceiling gas layer is found by solving the ordinary differential equation obtained from the law of conservation of energy for the near-ceiling gas layer:

$$\frac{dz_{l.b.}}{d\tau} = - \frac{G_{l.b.}}{\rho_0 F_c} - \frac{Q_{fire}(1-\phi)}{c_p \rho_0 T_0 F_c}. \quad (6)$$

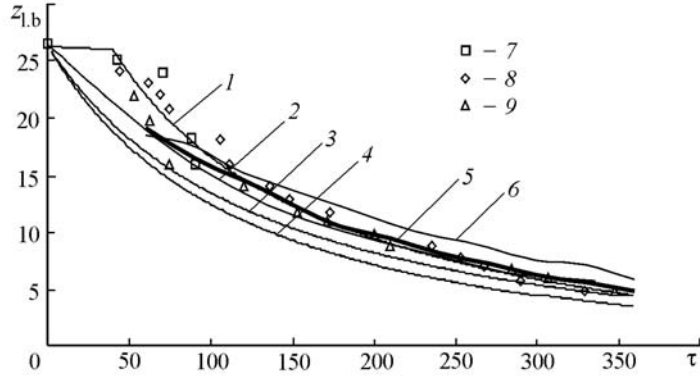


Fig. 2. Time dependence for the lower boundary of the near-ceiling layer: 1) Eq. (5), 2) approximation from [9], 3) Eqs. (3) and (4), 4) Eq. (1), 5) field model ($N = 15\%$), 6) field model ($N = 30\%$); experiment [9]: 7) determination based on density, 8) based on temperature, and 9) based on optical density.
 $z_{l.b.}$, m; τ , s.

The initial condition (at $\tau = 0$) is of the form $z_{l.b.} = H - \delta$. Equation (6) is solved by the Runge–Kutta method of the 4th order of accuracy. The bulk temperature and density in the near-ceiling gas layer are found by solving the differential equation of the law of conservation of mass of the near-ceiling gas layer and the equation of state of an ideal gas, respectively,

$$V \frac{d\rho_2}{d\tau} = G_{l.b.} - G_{i.g.}, \quad (7)$$

$$p_2 \approx p_0 = \rho_2 R T_2. \quad (8)$$

Field (Differential) Model of Calculating Heat and Mass Transfer. Use is made of a field calculational method developed in [7]. The generalized differential equation is of the form [7]

$$\frac{\partial}{\partial \tau} (\rho \Phi) + \operatorname{div} (\rho w \Phi) = \operatorname{div} (\tilde{A} \operatorname{grad} \Phi) + S. \quad (9)$$

Radiative heat transfer is determined using a moments method (diffusional model). The radiation component of the source term in the energy equation is

$$S_r = -\frac{4\pi}{3} \left(\frac{\partial^2 I}{\partial x^2} + \frac{\partial^2 I}{\partial y^2} + \frac{\partial^2 I}{\partial z^2} \right), \quad (10)$$

where the radiation intensity is found from the solution of the equation

$$\frac{1}{\beta} \left(\frac{\partial^2 I}{\partial x^2} + \frac{\partial^2 I}{\partial y^2} + \frac{\partial^2 I}{\partial z^2} \right) = 3\upsilon (I - I_{b.b.}). \quad (11)$$

Local values of the emission and absorption coefficients of radiation energy are determined using local values of the optical density of smoke [7]. The combustion reaction is viewed as single-step and irreversible:



The rate of reaction (12) with account for the effect of turbulence exerted on it (a diffusional-vortex model) is

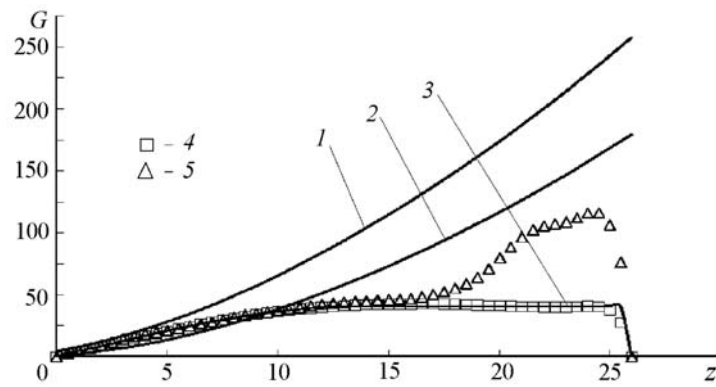


Fig. 3. Mass-flow-rate distributions over the atrium height: 1) Eq. (1), 2) Eqs. (3) and (4), 3) Eq. (5); numerical experiment (after 360 s): 4) over the cross section of the convective column, 5) over the entire cross section of an atrium parallel to the floor. G , kg/s; z , m.

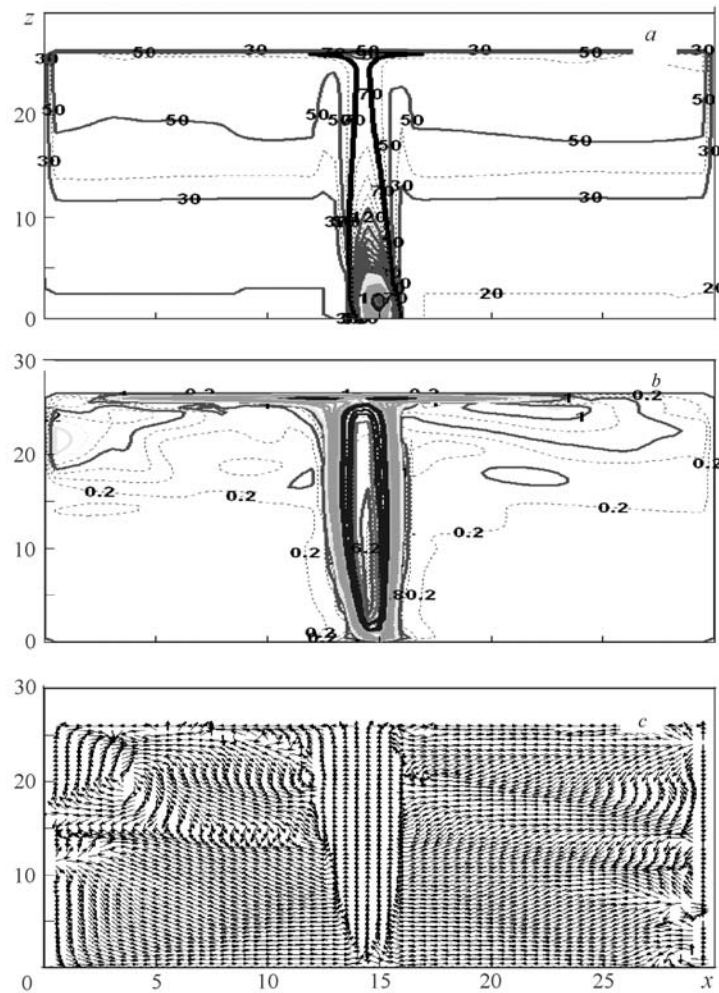


Fig. 4. Fields of temperatures (a) and velocities (b), and flow diagrams (c) in the longitudinal section of an atrium passing through the source of combustion, within 180 s of the beginning of a fire. z , x , m.

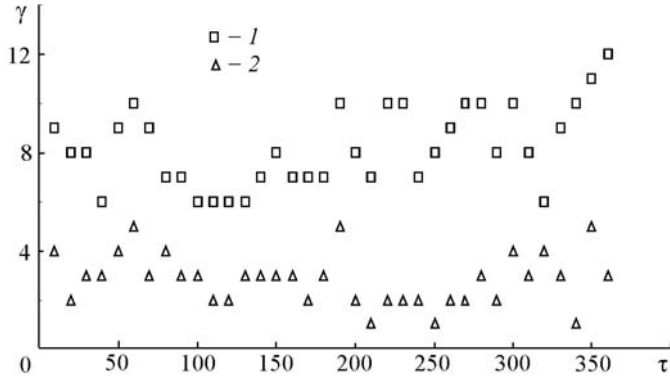


Fig. 5. Semivertex angle of a conical part of the convective column as a function of the time that elapsed from the beginning of combustion obtained using a field model: 1) maximum values; 2) minimum values. γ , rad; τ , s.

$$J_{c,r} = \rho \frac{\varepsilon}{k} \sin \left\{ 4X_{c,p}; 4 \frac{X_{O_2}}{s}; 2 \frac{X_{m,p}}{s+1} \right\}. \quad (13)$$

The initial and boundary conditions are presented in detail in [7]. Equations (9) and (11) are solved using a control volume approach [8] by an implicit finite-difference scheme on a uniform checkered grid.

Results of Numerical Experiment and Their Analysis. In study [9] a review is given of the results of full-scale experiments to determine the height of the lower boundary of the near-ceiling gas layer (the height of the zone not filled with smoke) and its bulk temperature in high rooms (higher than 6 m) in free development of a fire.

Figure 2 presents respectively calculated and experimental [9] time dependences of the height of the lower boundary of the near-ceiling gas layer (height of the zone not filled with smoke) and its bulk temperature in a conventionally hermetic room measuring $30 \times 24 \times 26.3$ m at the heat power $Q_{\text{fire}} = 1.3$ MW.

In a field model, use was made of a finite-difference grid measuring $61 \times 49 \times 54$ points. Here the position of the lower boundary of the near-ceiling layer was determined from the condition that the temperature rise is $N = 15$ and 30% (difference between the temperature on the lower boundary and the initial temperature in the room) of the maximum temperature rise in the near-ceiling layer (difference between the maximum temperature of the layer and the initial air temperature in the room) (rule of N percent [9]).

Characteristic distributions of mass flow rates averaged over the cross sections of the convective column along the room height are shown in Fig. 3. Figure 4 presents characteristic fields of temperatures ($^{\circ}\text{C}$) and velocities (m/s), as well as flow diagrams in the longitudinal section of an atrium, which passes through the source of combustion, within 180 s of the beginning of a fire.

From Fig. 4 it is seen that the shape of the convective column formed above the source of combustion is conical up to about half of the room height and is cylindrical above it.

Figure 5 gives dependences of the semivertex angle of a conical part of the convective column on the time that elapsed from the beginning of combustion, which were obtained using a field model as a result of the analysis of velocity fields in the longitudinal and cross sections of an atrium.

Figure 6 presents dependences of the height from the floor level on the time that elapsed from the beginning of combustion for a diverging conical part of the convective column, which were obtained using a field model as a result of the analysis of velocity fields in the longitudinal and cross sections of an atrium. Figure 6 also gives a time variation of the height from the floor starting with which the mass flow rate over the cross section of the column does not increase any longer.

From Fig. 2 it is seen that Eqs. (1), (3), and (4) (curves 2, 3, and 4) markedly overstate the velocity of descent of the lower boundary of the near-ceiling layer in comparison with experimental data, especially at the initial stage of a fire (within up to 50 s of the beginning of combustion). The error in determining the height of the lower boundary of the layer is in this case as large as 38%. Here, in accordance with Eq. (2), temperatures of the gas mixture over the cross section of the column will be lower than in experiment because of the large values of flow rates.

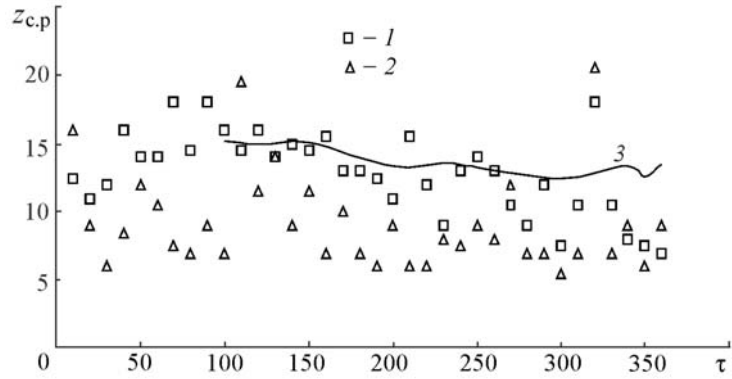


Fig. 6. Level of the floor of a divergent part of the column vs. time that elapsed from the beginning of combustion, obtained using a field model: 1) maximum values; 2) minimum values; 3) based on a constant mass flow rate. $z_{\text{con},p}$, m; τ , s.

This will lead to an underestimation of the fire danger, since the temperature of the near-ceiling gas layer will correspondingly be understated.

Equation (5) with allowance for the height of a conical part of the column (Fig. 6) and for the shape of the convective column (Fig. 5, the semivertex angle of the column), which are determined using a field model, qualitatively adequately reflects the dynamics of the layer descent at all fire stages. Results calculated using Eq. (5) (curve 1, Fig. 2) agree with experimental data with an error no larger than 25%. The difference between the flow rates determined using differential equation (5) (curve 3, Fig. 3) and a field model (curve 4, Fig. 3) does not exceed 3% over the entire atrium height.

The flow rates obtained from Eq. (1) (curve 1, Fig. 3) differ from the corresponding values obtained using a field model by no more than 19% up to the height $z = 5$ m. For $z > 5$ m, the difference can be as large as 540%. Compared to the calculations by a field model, expressions (3) and (4) (curve 2, Fig. 3) understate the flow rates by no more than 42% for $z < 10$ m and overstate the corresponding values by up to 340% for $z > 10$ m.

Thus, the use of the approximation of unlimited free convection in a fire in an atrium is correct only in the lower part of the convective column [in the considered example, for $\bar{z} < 0.4$ (see Fig. 3)].

It should be noted that, outside the column region in the upper part of an atrium, in the near-ceiling layer there are regions where the gas-mixture motion has a projection directed upward (see Fig. 3, curve 5, and Fig. 4c).

CONCLUSIONS

- When using a zone approach to modeling dynamics of the descent of the lower boundary of the near-ceiling gas layer in atria it is necessary to take account of the shape of the convective column formed above the source of combustion.
- The approximation of an unrestricted buoyant plume used for describing parameters of the convective column does not reflect the actual thermal gasdynamic picture of the fire development and can lead to both an underestimation and an overestimation of the fire danger of atria.
- The refinement of Eq. (5) [the effect of enclosing structures of a room (free convection in a limited volume) and of losses due to turbulent and laminar friction] calls for additional numerical studies using a field model [7] or for a physical experiment.

NOTATION

$$A = \frac{T_0 R^2}{g p_o^2 \pi^2}, \text{ dimensional parameter, } \text{s}^2 \cdot \text{m}^5 / (\text{kg}^2 \cdot \text{K}); B = \frac{Q_{\text{fire}}(1-\chi)}{z_{\text{fl}} c_p}, \text{ dimensional parameter, } \text{kg} \cdot \text{K} / (\text{m} \cdot \text{s}); c_p,$$

specific heat at constant pressure for a gas mixture in the convective column, J/(kg·K); F_c , area of the atrium ceiling,

m^2 ; g , acceleration due to gravity, m/s^2 ; G , rate of flow of gases through the plume section at a distance z from the surface of a combustible material along the height, kg/s ; $G_{in,a}$ and $G_{i,g}$ mass flow rates of the incoming air and issuing gases in natural gas exchange, kg/s ; $G_{l,b}$, mass flow rate of a gas mixture arriving at the near-ceiling zone from the convective column, kg/s ; H , room height, m ; I , radiation intensity, W/m^2 ; $I_{b,b} = \sigma T^4$, radiation intensity of an ideal blackbody, W/m^2 ; $J_{c,r}$, mass rate of the combustion reaction in unit volume of the gas medium, $kg/(s \cdot m^3)$; k , kinetic turbulence energy, m^2/s^2 ; N , percent of the temperature rise in the near-ceiling gas layer of the maximum temperature rise in the indicated layer; p_0 , pressure of the outside air at $z = 0$, Pa ; p_2 , volume-average pressure in the near-ceiling layer, Pa ; Q_{fire} , rate of heat release, W ; Q_{w1} , Q_{w2} , Q_c , and Q_{floor} , heat fluxes removed to the walls (below and above the lower boundary of the near-ceiling layer), ceiling, and floor, respectively, W ; r , radius of the surface of a combustible material, m ; R , gas constant of air, $J/(kg \cdot K)$; s , factor in the equation of combustion reaction; S , source term for Φ ; S_r , radiation component of the source term in the energy equation, W/m^3 ; T , temperature, K ; $T_{av,col}$, average temperature in the cross section of the convective column, K ; T_0 , temperature of the outside air, K ; T_2 , bulk temperature of the near-ceiling layer, K ; V , room volume, m^3 ; w , velocity of a gas mixture, m/s ; W_{for} and W_{sm} , volumetric flow rates of forced ventilation and smoke removal, m^3/s ; $X_{c,p}$, X_{O_2} , and $X_{m,p}$, mass concentrations of combustion products, oxygen, and products of gasification of a combustible material, respectively; x , y , and z , coordinates along the room length, width, and height, respectively, m ; $\bar{z} = z/H$, relative coordinate over the height of the cross section of the column, m ; $z_{con,p}$, height of a conical part of the convective column, m ; $z_{l,b}$, distance between the open surface of a combustible material and the lower boundary of the near-ceiling layer, m ; z_{fl} , height of the flame zone, m ; $z_{f,s}$, distance between the fictitious heat source and the surface of a combustible material, m ; β , total coefficient of radiation attenuation, $1/m$; Γ , diffusion coefficient for Φ ; γ , semivertex angle of the convective column, rad ; δ , thickness of a combustible material, m ; ϵ , dissipation rate of kinetic turbulent energy, m^2/s^3 ; Π , conventional chemical formula of combustion products; ρ , local density of a gas mixture, kg/m^3 ; ρ_0 , density of the outside air, kg/m^3 ; ρ_2 , average volume density in the near-ceiling layer, kg/m^3 ; σ , radiation constant of an ideal blackbody, $W/(m^2 \cdot K^4)$; T , conventional chemical formula of a combustible material; τ , time, s ; ν , total radiation coefficient, $1/m$; Φ , dependent variable (enthalpy of a gas mixture, velocity projections on coordinate axes, concentrations of components of a gas mixture (O_2 , CO , CO_2 , N_2 , and products of gasification of a combustible material), optical density of smoke, and kinetic turbulent energy and its dissipation rate); $\varphi = (Q_{w1} + Q_{w2} + Q_{floor})/Q_{fire}$, heat-loss coefficient; $\chi = Q_{w1}/Q_{fire}$, portion of heat released in the combustion center that comes to the enclosure; Ψ , mass rate of gasification of a combustible material, kg/s . Subscripts: O_2 , oxygen; sm , smoke removal; i,g , gases issuing to the outside through openings; col , column; con,p , conical part of the convective column; l,b , lower boundary of the near-ceiling gas layer; c , ceiling; in,a , air arriving at a room through the opening; c,p , combustion products; fl , flame zone; m,p , products of gasification of a combustible material; $fire$, fire; $floor$, atrium floor; for , forced ventilation; r , radiation; c,r , combustion reaction; av , average value; $w1$, walls below the lower boundary of the near-ceiling layer; $w2$, walls above the lower boundary of the near-ceiling layer; f,s , fictitious heat source; b,b , ideal blackbody; 0 , outside air; 2 , parameters of the near-ceiling layer.

REFERENCES

1. S. V. Puzach, Modified zonal model for calculating the thermodynamics of the gas in a fire within an atrium, *Inzh.-Fiz. Zh.*, **80**, No. 2, 84–89 (2007).
2. S. V. Puzach and E. S. Abakumov, Modified zonal model for calculating heat and mass transfer in a fire within an atrium, *Pozharovzryvobezopasnost'*, **16**, No. 1, 53–57 (2007).
3. Yu. A. Koshmarov, *Prediction of Dangerous Factors of Fire in a Room* [in Russian], Academy of State Fire-Prevention Service of the Ministry of Internal Affairs of Russia, Moscow (2000).

4. V. I. Prisadkov, V. V. Litskevich, and A. V. Fedorinov, Numerical methods of investigation of fire hazards for atria, *Pozharnaya Bezopasnost'*, No. 2, 64–70 (2002).
5. D. Drysdale, *Introduction to Fire Dynamics* [Russian translation], Stroizdat, Moscow (1988).
6. NFPA 92B. *Standard for Smoke Management Systems in Malls, Atria, and Large Spaces* (2005).
7. S. V. Puzach, *Methods to Calculate Heat and Mass Transfer in a Room Fire and Their Application to Solving Practical Problems of Fire and Explosion Safety* [in Russian], Academy of State Fire-Prevention Service of the Ministry for Emergency Situations of Russia, Moscow (2005).
8. S. Patankar, *Numerical Methods for Solving Problems of Heat Transfer and Fluid Dynamics* [Russian translation], Energoatomizdat, Moscow (1984).
9. K. Matsuyama, K. Misawa, and Y. T. Wakamatsu, Closed-form equations for room smoke filling during an initial fire, *Fire Sci. Technol.*, 1999. Vol. 19, No. 1. Pp. 27–38.